Atmos. Chem. Phys. Discuss., 11, 31067–31090, 2011
www.atmos-chem-phys-discuss.net/11/31067/2011/
doi:10.5194/acpd-11-31067-2011

Atmospheric Chemistry and Physics Discussions

Measurements of the movement of the jet streams at mid-latitudes, in the Northern and Southern Hemispheres, 1979 to 2010

R. D. Hudson

Departament of Atmospheric and Oceanic Science, University of Maryland, College Park, MD, 20742–2425, USA

Received: 22 August 2011 – Accepted: 4 November 2011 – Published: 22 November 2011

Correspondence to: R. D. Hudson (hudson@atmos.umd.edu)

Published by Copernicus Publications on behalf of the European Geosciences Union.

Abstract

Previous studies have shown that the mean latitude of the subtropical jet streams in both hemispheres have shifted toward the poles over the last few decades. This paper presents a study of the movement of both the subtropical and Polar fronts, the location of the respective jet streams, between 1979 and 2010 at mid-latitudes, using total ozone measurements to identify the sharp horizontal boundary that occurs at the position of the fronts. Previous studies have shown that the two fronts are the boundaries of three distinct regimes in the stratosphere, corresponding to the Hadley. Ferrel, and Polar meridionally overturning circulation cells in the troposphere, each of which has a distinct temperature profile. Over the period of study the horizontal area of the Hadley cell has increased at latitudes between 20 and 60 degrees while the area of the Polar cell has decreased. A linear regression analysis was performed to identify the major factors associated with the movement of the subtropical jet streams. These were: (1) changes in the Tropical land/ocean temperature, (2) direct radiative forcing from greenhouse gases in the troposphere, (3) changes in the temperature of the lower Tropical stratosphere, (4) the Quasi-Biennial Oscillation, and (5) volcanic eruptions. The dominant mechanism was the direct radiative forcing from greenhouse gases. Over the period of study the poleward movement of the subtropical jet streams was 3.7 ± 0.3 degrees in the Northern Hemisphere and 6.5 ± 0.2 degrees in the Southern Hemisphere, with a net expansion of the Tropical belt of 10.2 degrees. Previous studies have shown that weather systems tend to follow the jet streams. The observed poleward movement in both hemispheres over the past thirty years represents a significant change in the position of the subtropical jet streams, which should lead to significant latitudinal shifts in the global weather patterns, temperatures, precipitation and the hydrologic cycle.

ACPD

11, 31067–31090, 2011

Measurements of the movement of the jet streams at mid-latitudes

R. D. Hudson

1 Introduction

The jet streams are narrow bands of fast, meandering near-tropopause winds that flow around the globe. They are classified in two categories, the subtropical jet, imbedded in the subtropical upper troposphere front which is found in the poleward edge of the Hadley circulation, and the Polar jet, imbedded in the upper troposphere Polar front which is located above the Polar front zone (Holton, 1992; Bluestein, 1993). The positions of the jet streams are important because synoptic scale disturbances tend to form in the regions of maximum and minimum jet stream wind speed, and to propagate eastward along tracks that follow the jet axis (Holton, 1992). Changes in jet stream locations can therefore cause changes in the storm tracks, the global weather patterns, temperatures, precipitation and the hydrologic cycle.

Figure 1 shows an image for 1 April 1990, of the total column ozone field obtained by the National Aeronautic and Space Administration (NASA) Total Ozone Monitoring Spectrometer (TOMS) on the Nimbus-7 satellite. Hudson et al. (2003) showed that, on any day, the total column ozone field could be used to identify the position of the subtropical and Polar upper tropospheric fronts, the location of the subtropical and Polar jet streams, respectively. The abrupt change in the tropopause height at the frontal boundaries is manifested by an abrupt change in the total column ozone. Hudson et al. (2003) developed a technique to calculate the total ozone value at the center of the two frontal boundaries from the total ozone daily images. They then used these ozone values to determine the position of the respective fronts. Hudson et al. (2003) showed good agreement between the position of their calculated fronts and those derived fron the NCEP/NCAR reanalysis (Kalnay, 1996; Kistler et al., 2001) using the potential vorticity on isentropic potential temperature surfaces. The position of the fronts derived from the ozone data are marked on Fig. 1 as solid lines, red (Polar front) and blue (subtropical front). The focus of the work reported here is on the net latitude movement of the two fronts as a surrogate for the poleward movement of the two jet streams.

Hudson et al. (2006), found that the total ozone value associated with the center of the frontal boundary on a particular day was constant with longitude, with a slight

ACPD
11, 31067–31090, 2011

latitude dependence. They were able to identify three distinct stratospheric regimes (Tropical, mid-latitude and Polar), separated by the subtropical and Polar fronts. Within each regime the total column ozone was almost constant, again with a slight latitude dependence (see Fig. 1). In the troposphere these regimes correspond to the Hadley, Ferrell and Polar meridional cells. Hudson et al. (2003) also showed, using rawinsonde measurements, that each regime had a distinct troposphere temperature profile. In addition, Follette-Cook et al. (2009), have shown that in the stratosphere each regime has a distinct ozone and water vapor profile below an altitude of about 25 km.

Hudson et al. (2006) examined the ozone trends within each regime and concluded that the area of the Tropical regime had increased over the period 1979 to 2003, equivalent to a northward movement of the subtropical front of about 3 degrees latitude. Fu et al. (2006) examined atmospheric temperature trends in the troposphere and stratosphere over the period from 1979 to 2005, and concluded that the subtropical jet stream in both hemispheres had shifted poleward by ~1 degree latitude in both the summer and winter seasons. Hu and Fu (2007) examined the time evolution of the zonal mean-meridional mass streamfunctions from three reanalysis data sets, and the outgoing long-wave radiation, between 1979 and 2005. The three data sets used were the ERA-40 (Uppala et al., 2005), NCEP/NCAR (Kalnay, 1996; Kistler et al., 2001), and NCEP/DOE (Kanamitsu et al., 2002) respectively. Hu and Fu (2007) obtained a value for the expansion of the Tropical belt (defined as the latitude separation of the southern and northern subtropical fronts) between 2 and 4.5 degrees latitude. Seidel and Randel (2007) examined changes in the tropopause height derived from rawinsonde measurements and the NCAR/NCEP and ERA-40 reanalysis data sets. They found that between 1979 and 2005 the Tropical belt widened from between 3 and 8 degrees latitude.

As noted above, the poleward movement of the fronts implies a movement of the jet streams, which in turn implies a poleward movement of the synoptic weather patterns leading to a change in climate. It is important to understand the nature of the poleward movement of the fronts and to identify the mechanisms that are associated with this

ACPD
11, 31067–31090, 2011

Measurements of the movement of the jet streams at mid-latitudes

R. D. Hudson

movement. This paper extends the analysis performed by Hudson et al. (2006) to both hemispheres for the time period 1979 to 2010. The study is confined to latitudes between the equator and 60°, the upper limit of 60 degrees being set by the spatial coverage of the total ozone data sets. A linear regression analysis is performed using selected climate indices that are believed to influence the movement of the fronts. Section 2 presents the sources of total ozone data used in the analysis. Section 3 outlines the method used to identify the frontal boundaries. Section 4 presents the analysis of the monthly mean equivalent latitudes, and Sect. 5 discusses the results of the analysis. Section 6 gives the conclusions of the paper.

2 Sources of the ozone data

In order to identify the frontal boundaries one needs daily total ozone images that cover the entire globe. The daily total ozone data used in this study were obtained from four instruments: (1) TOMS on the Nimbus-7 satellite (N7-TOMS: McPeters et al, 1996), for 1979–1994 (2) TOMS on the Explorer satellite (EP-TOMS: McPeters et al., 1998) for 1996–2006, (3) Ozone Monitoring Instrument on the AURA satellite (OMI: Bhartia et al., 2002) for 2004 to present, and (4) The Advanced Tiros-N Operational Vertical Sounder which produces the TOVS data set (Neuendorfer, 1996) for 1980 to present. The latter data set is retrieved from several National Oceanic and Atmospheric Administration (NOAA) low Earth orbit satellites using infrared radiance measurements made by the High Resolution Infrared Sounder (HIRS) at a wavelength of 9.6 microns. The TOVS data set is not archived by NOAA before 2002: for the time period 1980 to 2001 the TOVS data set produced by Muller et al. (2002) was used.

The TOMS instruments have a spatial resolution of 1.0° latitude by 1.25° longitude, while the OMI and TOVS instruments have a spatial resolution of 1.0° latitude by 1.0° longitude. All of the instruments have missing data above 60° latitude during the Polar night. The TOMS and OMI instruments obtain total ozone from measurements of the backscatter of solar ultraviolet radiation from the atmosphere and as such do not get

ACPD
11, 31067–31090, 2011

results during the Polar night. The TOVS data sets have a problem in the winter months when the Polar vortex is formed. The low values of total ozone that accompany the vortex cannot be resolved by the TOVS algorithms and are listed as missing data. For this reason the analysis of the frontal movement is limited to latitudes below 60°.

There is a bias between the total ozone values obtained by the four instruments, which is a function of latitude, and/or total ozone amount. The TOVS data are about two per cent lower than the TOMS data, the exact amount depending on the particular instruments used, while the OMI data are about one per cent higher. A correction is applied to the TOVS and OMI data sets on a daily basis as a function of latitude to provide a consistent overall data set.

3 Determination of the ozone boundaries

The method used to determine the latitude and longitude of the fronts for each day from the total ozone data is described in Hudson et al. (2003, 2006). In 2005 EP-TOMS, TOVS and OMI overlap in their data coverage. Figure 2 compares the derived values of total ozone that correspond to the boundaries of the fronts for the eleventh day of March, June, September, and December of 2005. The agreement between the values from each instrument is excellent, and the differences shown in Fig. 2 lead to a maximum error in the determination of the mean latitude of 0.2 degrees, which is less than the spatial resolution of the instruments. The actual boundary used in the analysis is the best fit to the data, shown as a solid line in Fig. 2. In general at least two instrument data sets are used to derive the average boundary, the exception being between 1993 and 1996, when TOVS was the only data set available.

The spatial resolution of the total ozone data introduces an error in the determination of the latitude and longitude of the fronts. However the area of each regime can be determined with much greater accuracy. The boundaries derived from the total ozone data were used to obtain the areas of the three regimes between the equator and 60 degrees latitude (see Hudson et al., 2003, 2006 for details). The areas were calculated

ACPD
11, 31067–31090, 2011

for each day, and then converted to an equivalent latitude. For the subtropical front, the equivalent latitude is defined as the latitude at which the zonal area from the equator to that latitude is equal to the area of the Tropical regime. For the Polar front, the area used is the sum of the Tropical and mid-latitude regimes. It should be noted that the equivalent latitude, as defined, is area weighted. Monthly mean equivalent laitude and the error of the mean were obtained from the daily data. Figure 3 shows the monthly mean equivalent latitude as a function of time from 1979 to 2010 for the two fronts for the Northern and Southern Hemispheres respectively. The upper latitude of 60°, determined by the measurements, imposes an artificial cap on the area of the Polar regime and hence on the monthly mean equivalent latitude of the Polar front, as is shown in Fig. 3. This limits the usefulness of the data in understanding the movement of the Polar front. The 60° limit also imposes a cap on the area of the Tropical regime, but the monthly mean equivalent latitude of the subtropical front is at 35°, and the impact is much smaller. The regression analysis has been applied only to the monthly mean equivalent latitude of the subtropical front.

4 Analysis of the monthly mean equivalent latitudes

Lu et al. (2009), studied the possible causes of the widening of the Tropical belt. They identified four mechanisms of forcing, (1) sea surface temperature, (2) direct radiative forcing from greenhouse gases in the troposphere, (3) temperature changes in the lower Tropical stratosphere due to radiative forcing, from greenhouses gases, volcanic aerosols, and changes in the stratospheric ozone concentration, and (4) variations in total solar irradiance (solar constant).

In order to quantify the contributions of each of these mechanisms the monthly mean equivalent latitude of the subtropical front was analyzed using a linear regression routine (Press et al., 1992). The errors determined from the daily equivalent latitudes were explicitly introduced into the routine. Four climate indices were used in the linear regression analysis; Tropical surface temperature (referred hereafter as

ACPD
11, 31067–31090, 2011

SST), radiative forcing in the troposphere (RADF), the lower stratosphere temperature in the tropics (TEMP) and the quasi-biennial oscillation (QBO). The SST used was the extended reconstruction sea surface temperature anomaly (ERSST.v3b, Smith et al., 2008) for both land and ocean covering the latitude range 0 to 30° N and 0 to 30° S. This index is based on measurements and should include any change in the solar constant. For RADF, the NOAA annual greenhouse gas index (AGGI, Hoffman et al., 2006) was used. The TEMP index chosen was the Tropical temperature anomaly based on rawinsonde measurements (RATPAC, Free et al., 2005). This data set lists results at several pressure levels. It was found that the data for 50 mb gave the best fit. As TEMP is based on measurements it should include the effect of volcanic eruptions, solar irradiance and radiative forcing in the lower stratosphere, and additional indices for these effects do not need to be included. The QBO index was obtained from the NOAA Physical Sciences Division, Earth System Research Laboratory (www.esrl.noaa.gov/psd/data/climareindices/list/{#}QBO), and is based on the zonal average of the 30 mb wind. Two seasonal terms (annual and semi-annual) are also included, each with a sine and a cosine component. The semi-annual term arises from changes in the solar irradiance at the equator which has a maximum at both the spring and autumnal equinox. The annual term reflects the movement of the inter-Tropical convergence zone (ITCZ) and solar irradiance at higher latitudes which has a maximum at the summer solstice. In order to get a good fit between the measured and the calculated data, especially for the Southern Hemisphere, the amplitude of the seasonal terms was assumed to have a dependence on RADF. In all eight terms were included in the analysis to represent the seasonal terms. The quantities used in the regression analysis to study the movement of the subtropical front were the change in the monthly mean equivalent latitude versus the change in the indices since January 1979.

Figure 4 shows the results of the regression analysis for the Northern and Southern Hemispheres. Each panel displays the measured data, the best fit from the regression analysis, and the difference between the measured data and the best fit. Table 1 gives

ACPD
11, 31067–31090, 2011

the values of the regression constants and their associated errors. The errors quoted are 2σ. Figure 5 shows a comparison between the best fit for each climate index compared to the residual obtained from a regression analysis performed without that climate index. From this figure one can obtain a visual image of the quality of the fit. It should be noted that when the particular climate index is added back to the regression the coefficients do change slightly. Figure 6 shows the contributions of each index to the overall fit for both hemispheres. Figure 7 shows the annual average fractional area of the three regimes from 1979 to 2010 for four latitude bands, 25°–30°, 35°–40°, 45°–50° and 55°–60°. Table 2 gives the slope of a linear fit (Press et al., 1992) to these fractional areas for each regime expressed as a percentage.

In order to calculate the overall movement of the subtropical fronts over the 32 yr time period, the effect of the seasonal and QBO terms, which are periodic, was first removed from the latitude data for each hemipshere. The results are shown in Fig. 8. The solid line in each panel of Fig. 8 is the result of a linear fit, including measurement errors (Press et al., 1992).

5 Discussion

5.1 Regression analysis

The difference plot for the Northern Hemisphere shown in Figure 4 shows a distinct rise after 1992. The sharp peak shows a strong corelation with the Mount Pinatubo eruption which occurred in June, 1991. A similar peak can be seen after the El Chichon eruption in April, 1982. A comparison with calculated values for the volcanic radiative forcing made by Ammann et al. (2003) shows good agreement with the shape of the difference plot, but with a lag between the radiative forcing and the movement of the front of 15 months.

As noted earlier the only seasonal terms of significance were the annual and semi-annual terms. The overall contribution of the seasonal term with a constant amplitude is shown in Fig. 6a and that for the amplitude proportional to RADF is shown in Fig. 6b.

ACPD

11, 31067–31090, 2011

Measurements of the movement of the jet streams at mid-latitudes

R. D. Hudson

Over the course of a year the range of the amplitude of the constant seasonal term is 7.8° in latitude for the northern subtropical front and 2.6 degrees for the southern subtropical front. In the Southern Hemisphere the range of the RADF dependent amplitude has increased by 7.1° from 1979 to 2010, while that for the Northern Hemisphere has increased by 1.4 degrees. For the Northern Hemisphere the maximum of the constant annual term occurs in January while for the Southern Hemisphere it occurs in November. The semi-annual term peaks in June and December in both the Northern and Southern Hemispheres. The maximim of the RADF dependent annual term occurs in August for the Northern Hemisphere, and March for the Southern Hemisphere. The RADF semi-annual term peaks in October and April in the Northern Hemisphere, August and February in the Southern Hemisphere. The sum of the seasonal terms peaks in November/December in the Northern Hemisphere and in March in the Southern Hemisphere.

Figures 5a and 6c show the dependence of the latitude of the subtropical front on the tropospheric radiative forcing. The effect is large and is positive. Over the period of the study the subtropical front has moved by 4.2° in the Northern Hemisphere and 6.9° in the Southern Hemisphere.

Figures 5b and 6d show the effect of temperature change in the lower stratosphere on the movement of the fronts. Over the past 30 yr effect has introduced a latitude shift of about 1° in the Northern Hemisphere and 1.5 degrees in the Southern Hemisphere. This implies that a cooling of the lower stratosphere moves the front towards the pole, in agreement with the theoretical analysis of Lu et al. (2009).

Figures 5c and 6e show the dependence of the frontal movement on the Tropical land and ocean mean temperature anomaly (0 to 30° latitude). An increase in the value of the SST leads to a decrease in the latitude of the subtropical front by about 2 degrees in the Southern Hemisphere and 0.5 degrees in the Northern Hemisphere. The latitude shift has the same sign as the results obtained by Lu et al. (2009). Figures 5d and 6f show the dependence on the QBO. There is a much stronger dependence in the Southern Hemisphere than in the Northern Hemisphere. An increase in the QBO leads

ACPD
11, 31067–31090, 2011

to an increase in the latitude of the subtropical front. Over a typical QBO cycle the front moves about 1.5° in the Northern Hemisphere, and 3.5° in the Southern Hemisphere.

5.2 Latitude bands

Figure 7 and Table 2 show that the fractional area of the Tropical regime has increased from 1979 to 2010 at all latitude bands in both hemispheres. The area of the mid-latitude regime in the Northern Hemisphere decreases below a latitude of 45 degrees, and increases above that latitude. In the Southern Hemisphere, the area of the mid-latitude regime decrerases at all latitudes. The area of the Polar regime decreases at all latitudes in both hemispheres, As noted before, Hudson et el. (2003), showed that each regime had a distinct troposphere temperature profile over a large latitude range. The global temperature changes discussed in the Intergovermental Panel on Climate Change 2007 assessment report, AR4 (IPCC, 2007) are based on zonal averages. Let the mean ground temperature within the latitude zone, for the Tropical regime be defined as T_t , for the mid-latitude regime as T_m and for the Polar regime as T_p. Then the mean zonal temperature, T, is given by:

$$T = T_t \times A_t + T_m \times A_m + T_p \times A_p \quad (1)$$

Where A_t, A_m and A_p are the fractional areas of the regimes within the latitude zone such that:

$$A_t + A_m + A_p = 1.0 \quad (2)$$

In general $T_t > T_m > T_p$ and thus an increase in A_t and a decrease in A_m and A_p will lead to an increase in T. This trend will contribute to the overall observed temperature trend.

6 Conclusions

Over the period of study the subtropical front has moved poleward by 3.7 ± 0.3 degrees in the Northern Hemisphere and 6.5 ± 0.2 degrees in the Southern Hemisphere.

ACPD
11, 31067–31090, 2011

The net expansion of the Tropical belt is 10.2 ± 0.6 degrees. For the shorter period from 1979 to 2005 the expansion is reduced to 8.3 degrees, at the upper limit of the range of 3–8 degrees obtained by Seidel and Randel (2007). A regression analysis has shown that the primary cause of the poleward movement of the fronts is radiative forcing in the tropics, in agreement with previous studies, IPCC (2007). Weather systems tend to follow the jet streams which are imbedded in the fronts. Hence a poleward movement of the fronts leads to a net movement of the weather patterns towards the poles. IPCC (2007), reports a shift in the storm track locations, increased storm activity accompanied by a decrease in storm numbers over the past thirty years. The observed poleward movement in both hemispheres over the past thirty years represents a significant change in the position of the subtropical jet streams, which should lead to significant latitudional shifts in the global weather patterns, temperatures, precipitation and the hydrologic cycle.

Acknowledgements. The author wishes to acknowledge helpful comments from M. Andrade, and T. Canty, who kindly agreed to read an earlier version of the manuscript. The author would also like to thank the editor for his helpful and insightful feedback.

References

Archer, C. and Caldiera, K.: Historical trends in the Jet Streams, Geophys. Res. Lett., 35, L08803, doi:10.1029/2008GL033614, 2008.

Amman, C. M., Meehl, G. A., Washington, W. M., and Zander, C. S.: A monthly and latitudionally varying volcanic forcing data set in simulations of the 20th century climate, Geophys. Res. Lett., 30, 1657, doi:10.1029/2003GL016875, 2003.

Bluestein, H. B.: Synoptic-Dynamic Meteorology in Midlatitudes, Vol. 2, Observations and Theory of Weather Systems, 594 pp., Oxford Univ. Press, New York, 1993

Follette-Cook, M. B., Hudson, R. D., and Nedoluha, G. E.: Classification of Northern Hemisphere stratospheric ozone and water vapor profiles by meteorological regime, Atmos. Chem. Phys., 9, 5989–6003, doi:10.5194/acp-9-5989-2009, 2009.

Free, M., Seidel, D. J., Angell, J. K., Lanzante, J., Durre, I., and Peterson, T. C.: Radiosonde At-

ACPD

11, 31067–31090, 2011

mospheric Temperature Products for Assessing Climate (RATPAC): A new data set of large-area time series, J. Geophys. Res., 110, D22101, doi:10.1029/2005JD006169, 2005.
Fu, Q., Johanson, C. M., Wallace, J. M., and Reichler, T.: Enhanced Mid-Latitude Tropospheric Warming in Satellite Measurements, Science, 312, 1179, doi:10.1126/science.1125566, 2006.
Hoffman D. J., Butler, J. H., Dlugokencky, E. J., Elkins, J. W., Masarie, K., Montzka, S. A., and Tans, P.: The role of carbon dioxide in climate forcing from 1979 to 2004: Introduction of the Annual Greenhouse Gas Index, Tellus B, 58, 614–619, 2006
Holton, J. R. An Introduction to Dynamic Meteorology, 511 pp., Elsevier, New York, 1992.
Hu, Y. and Fu, Q.: Observed poleward expansion of the Hadley circulation since 1979, Atmos. Chem. Phys., 7, 5229–5236, doi:10.5194/acp-7-5229-2007, 2007.
Hudson, R. D., Andrade, M., Follette, M. B., and Frolov, A. D.: The total ozone field separated into meteorological regimes – Part I: Defining the regimes, J. Atmos. Sci., 62, 1669–1677, 2003.
Hudson, R. D., Andrade, M. F., Follette, M. B., and Frolov, A. D.: The total ozone field separated into meteorological regimes - Part II: Northern Hemisphere mid-latitude total ozone trends, Atmos. Chem. Phys., 6, 5183–5191, doi:10.5194/acp-6-5183-2006, 2006.
IPCC: Climate Change 2007; The Physical Science Basis, Contribution of Working Group 1 to the Fourth Assessment Report of the Intergovermental Panel on Climate Change, edited by: Solomon, S., Qui, D., Manning, M., Chen, Z., Marquis, M., Avery, K. B., Tigner, M., and Miller, H. L., Cambridge University press, Cambridge UK and New York, NY, USA, 996 pp., 2007.
Kanamitsu, M., Ebisuzak, W., and Woollen, J.: NCEP-DOE AMPII reanalysis (R-2), B. Am. Meteorol. Soc., 83, 1631–1641, 2002.
Kaffel, A. K. and Muller, M. J.: Results of neural network total ozone retrieval on global NOAA_TOVS data, Technical Proceedings of the 10th International ATOV Study Conference, edited by: La Marshall, J. and Jasper, J. D., Bureau of Meteorology Research Centre, Melbourne, Australia, 268–275, 1999.
Kalnay, E., Kanamitsu, M., Kistler, R., Collins, W., Deaven, D., Gandin, L., Iredell, M., Saha, S., White, G., Woollen, J., Zhu, Y., Chelliah, M., Ebisuzaki, W., Higgins, W., Janowiak, J., Mo, K. C., Ropelewski, C., Wang, J., Leetmaa, A., Reynolds, R., Jenne, R., and Joseph, D.: The NMC/NCAR 40 Yr Reanalysis Project, B. Am. Meteor. Soc., 77, 437–471, 1996.
Kistler, R., Kalnay, E., Collins, W., Saha, S., White, G., Woollen, J., Chelliah, M., Ebisuzaki, W.,

Kanamitsu, M., Kousky, V., van den Dool, H., Jenne, R., and Fiorino, M.: The NCEP-NCAR 50 Yr Reanalysis: Monthly Means CD-ROM and Documentation, B. Am. Meteor. Soc., 82, 247–268, 2001.

Lu, J., Deser, C., and Reichler, T.: Cause of the widening of the Tropical belt since 1958, Geophys. Res. Lett., 36, L03803, doi:10.1029/2008GL036076, 2009.

McPeters, R., Bhartia, P. K., Kruger, A., Herman, J., Schlesinger, B., Wellermeyer, C., Seftor, C., Jaross, G., Taylor, S., Swissler, T., Torres, O., Byerly, W., and Cebula, R.: Nimbus-7 Total Ozone Mapping Spectrometer (TOMS) Data Products User's Guide, NASA Reference Publication 1384, National Aeronautic and Space Administration, Washington, DC, 1996.

McPeters, R., Bhartia, P. K., Kruger, A., Herman, J., Wellermeyer, C., Serafino, C., Jaross, G., Torres, O., Moy, L., Labow, G., Byerly, W., Taylor, S., Swissler, T., and Cebula, R.: Earth Probe Total Ozone Mapping Spectrometer (TOMS) Data Products User's Giude, NASA Technical Report TR_1998-206895, National Aeronautic and Space Administration, Washington, DC, 1998.

Neurenforfer, A, M.: Ozone monitoring with TIROS-N operational vertical sounders, J. Geophys. Res., 101, 18807–18828, 1996.

Press, W. H., Teuskojsky, S. A., Vettering, W. T., and Flannering, B. P.: Numerical recipes in C, 960 pp., Cambridge University Press, New York, USA, 1992.

Seidel, D. and Randel, W. J.: Recent widening of the Tropical belt: Evidence from Tropical observations, J. Geophys. Res., 112, D20113, doi:10.1029/2007JD008861, 2007.

Smith, T. M., Reynolds, R. W., Petersen, T. C., and Lavrinmore, J.: Improvements to NOAA's Historical Merged Land-Ocean Surface Temperature Analysis (1880 to 2006), J. Climate, 21, 2283–2296, 2008.

Uppala, S. M., Kållberg, P. W., Simmons, A. J., Andrae, U., da Costa Bechtold, V., Fiorino, M., Gibson, J. K., Haseler, J., Hernandez, A., Kelly, G. A., Li, X., Onogi, K., Saarinen, S., Sokka, N., Allan, R. P., Andersson, E., Arpe, K., Balmaseda, M. A., Beljaars, A. C. M., van de Berg, L., Bidlot, J., Bormann, N., Caires, S., Chevallier, F., Dethof, A., Dragosavac, M., Fisher, M., Fuentes, M., Hagemann, S., Hólm, E., Hoskins, B. J., Isaksen, L., Janssen, P. A. E. M., Jenne, R., McNally, A. P., Mahfouf, J.-F., Morcrette, J.-J., Rayner, N. A., Saunders, R. W., Simon, P., Sterl, A., Trenberth, K. E., Untch, A., Vasiljevic, D., Viterbo, P., and Woollen, J.: The ERA-40 re-analysis, Q. J. Roy. Meteorol. Soc., 131, 2961–3012, 2005.

Table 1. Constants of the regressions analysis for the Northern and Southern Hemispheres. The errors are 2σ.

Index	Constant-N	Error-N	Constant-S	Error-S
Temperature	−1.1	0.2	−.72	0.07
Radiative forcing	3.6	0.5	5.2	0.3
SST	−2.6	0.6	−4.9	0.4
QBO	.047	.008	.12	.05
Sin(ϖt)	0.50	0.15	−1.0	0.2
Cos(ϖt)	3.8	0.3	0.92	0.2
Sin(2ϖt)	−0.6	0.3	−.04	0.2
Cos(2ϖt)	0.48	0.3	0.10	0.18
RADF* Sin(ϖt)	−0.43	0.4	3.3	0.3
RADF* Cos(ϖt)	−0.48	0.4	0.69	0.3
RADF* Sin(2ϖt)	−0.40	0.4	0.68	0.3
RADF* Cos(2ϖt)	−0.33	0.5	0.30	0.3

ACPD
11, 31067–31090, 2011

Measurements of the movement of the jet streams at mid-latitudes

R. D. Hudson

Table 2. Increase/decrease of the area of the regimes for the Northern and Southern Hemisphere for 5 degree latitude bands between 25 and 60°. The change is expressed as the per cent change per decade. The errors are 2σ.

Latitude band	Regime	North % Change/Dec	Error	South % Change/Dec	Error
25–30	Tropical	2.43	0.28	2.95	.22
	Midlatitude	−3.11	0.22	−4.16	.16
	Polar				
30–35	Tropical	5.17	.30	5.96	.26
	Midlatitude	−4.25	.26	−6.48	.24
	Polar				
35–40	Tropical	5.26	.24	5.80	.24
	Midlatitude	−1.8	.28	−4.58	.26
	Polar	−0.96	.10	−1.48	.06
40–45	Tropical	3.82	.20	4.06	.24
	Midlatitude	−.451	.28	−2.82	.29
	Polar	−2.67	.18	−2.04	.12
45–50	Tropical	2.57	.16	4.00	.24
	Midlatitude	1.40	.30	−1.92	.28
	Polar	−3.29	.24	−3.51	.18
50–55	Tropical	3.53	.12	5.05	.20
	Midlatitude	2.48	.30	.092	.28
	Polar	−4.62	.14	−4.83	.24
55–60	Tropical	4.08	.11	5.96	.22
	Midlatitude	2.05	.32	.02	.30
	Polar	−3.79	.30	−8.29	.24

ACPD
11, 31067–31090, 2011

Measurements of the movement of the jet streams at mid-latitudes

R. D. Hudson

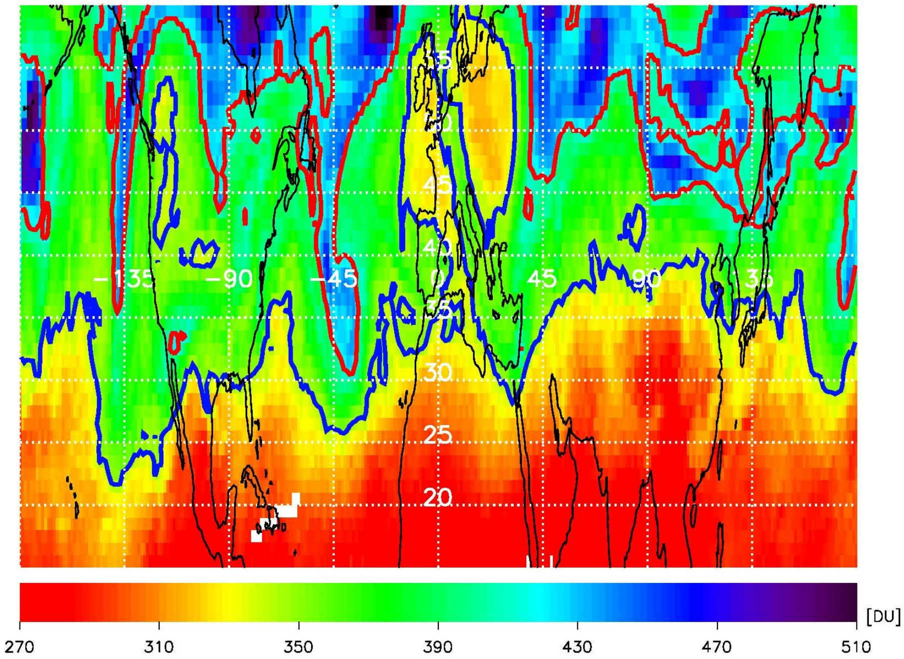

Fig. 1. Total ozone image for 1 April 1990, from the TOMS instrument on the Nimbus-7 satellite. The solid blue line shows the location of the subtropical front (subtropical jet stream), while the solid red line shows the location of the Polar front (Polar jet stream). The units of the color bar are Dobson Units (1 DU = 1 millimeter atmospheres^{-1}).

ACPD
11, 31067–31090, 2011

Measurements of the movement of the jet streams at mid-latitudes

R. D. Hudson

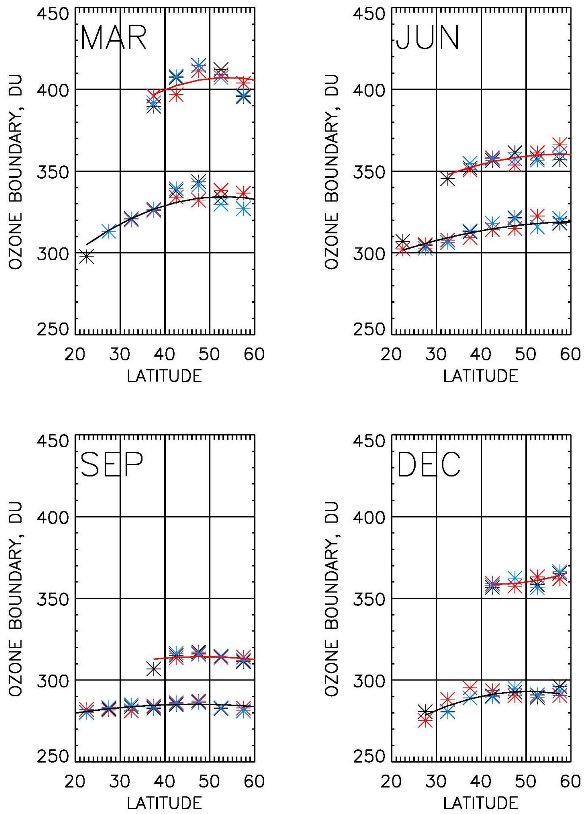

Fig. 2. Derived ozone boundaries from TOMS (red stars), TOVS (blue stars), and OMI (black stars). Data used is for the Northern Hemisphere on the 11th of each month in 2005. On each panel the upper set is for the Polar front, the lower set is for the subtropical front. The solid line is the best fit, using all three instruments, for the subtropical front (black) and the Polar front (red).

ACPD
11, 31067–31090, 2011

Measurements of the movement of the jet streams at mid-latitudes

R. D. Hudson

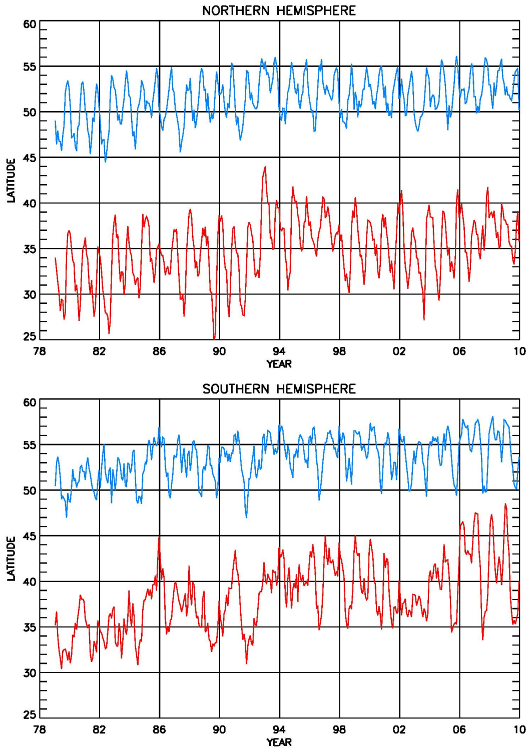

Fig. 3. Monthly mean equivalent latitude of the subtropical and Polar fronts for the Northern Hemisphere (upper panel) and the Southern Hemisphere (lower panel) for the region between the equator and 60° latitude.

ACPD
11, 31067–31090, 2011

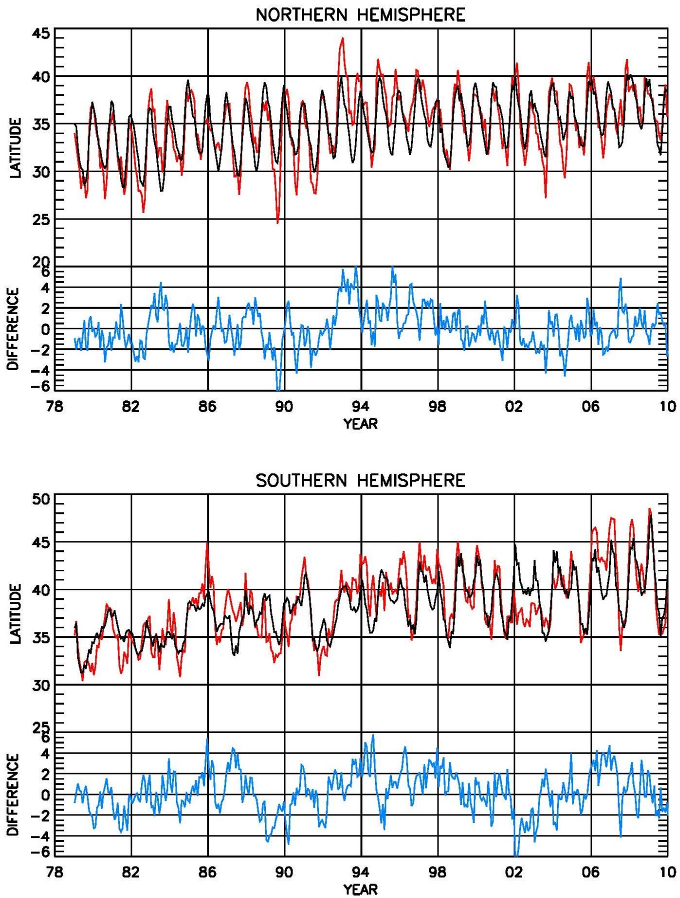

Fig. 4. Comparison of the measured monthly mean equivalent latitude of the subtropical front (red line) and the best fir from the regression analysis (black line) for the Northern and Southern Hemispheres. The blue line is a plot of the difference (measured minus the best fit).

ACPD
11, 31067–31090, 2011

Measurements of the movement of the jet streams at mid-latitudes

R. D. Hudson

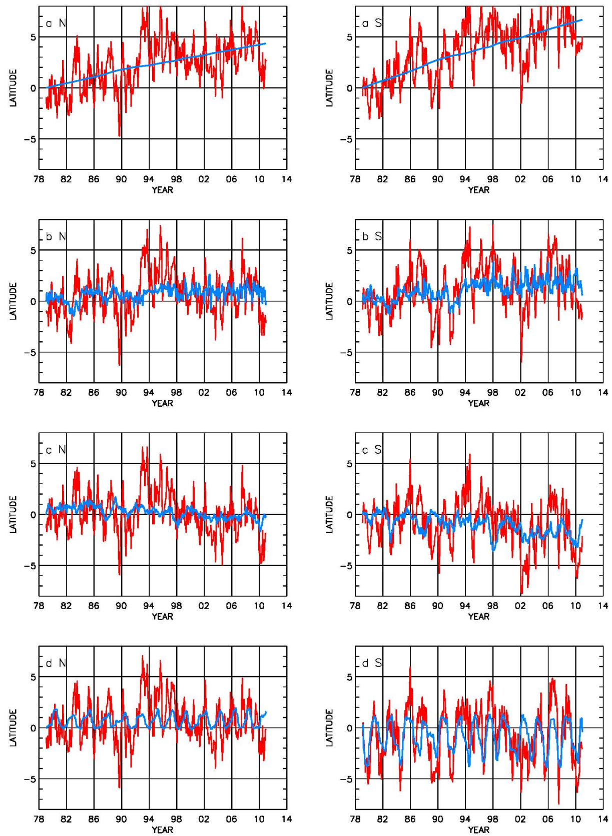

Fig. 5. Comparison between the best fit (blue line) for each climate index compared to the residual (red line) obtained from a regression analysis of the monthly mean equivalent latitude performed without that climate index: **(a)** (N and S) for RADF, **(b)** (N and S) for TEMP, **(c)** (N and S) for SST, and **(d)** (N snd S) for QBO.

ACPD
11, 31067–31090, 2011

Title Page
Abstract | Introduction
Conclusions | References
Tables | Figures
◀| |▶
◀ ▶
Back | Close
Full Screen / Esc
Printer-friendly Version
Interactive Discussion

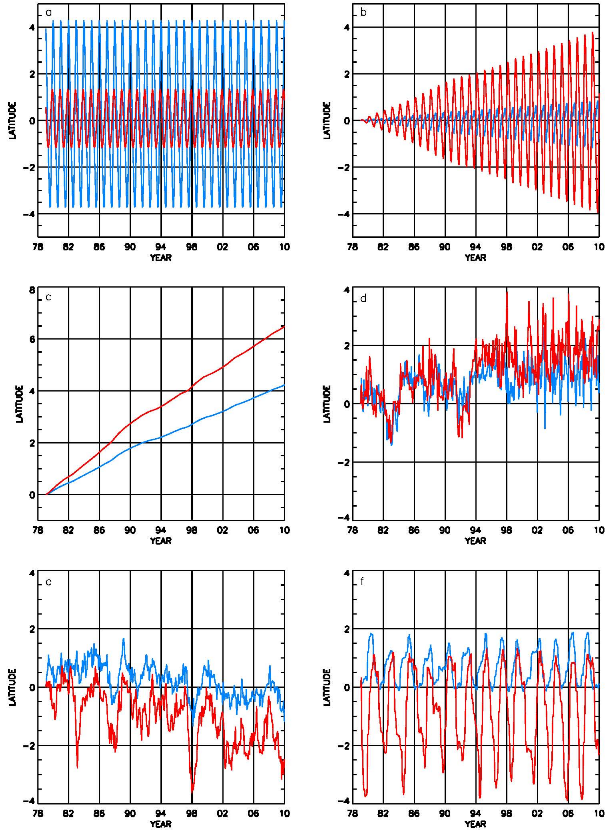

Fig. 6. Contribution of each climate index to the monthly mean equivalent latitude. The red lines are the results for the Southern Hemisphere, the blue for the Northern Hemisphere: **(a)** results for the constant seasonal terms, **(b)** results for the time dependent, seasonal terms **(c)** results for the RADF index, **(d)** results for the TEMP index, **(e)** results for the SST index, **(f)** results for the QBO index.

ACPD
11, 31067–31090, 2011

Measurements of the movement of the jet streams at mid-latitudes

R. D. Hudson

Title Page
Abstract | Introduction
Conclusions | References
Tables | Figures
◀| |▶
◀ ▶
Back | Close
Full Screen / Esc
Printer-friendly Version
Interactive Discussion

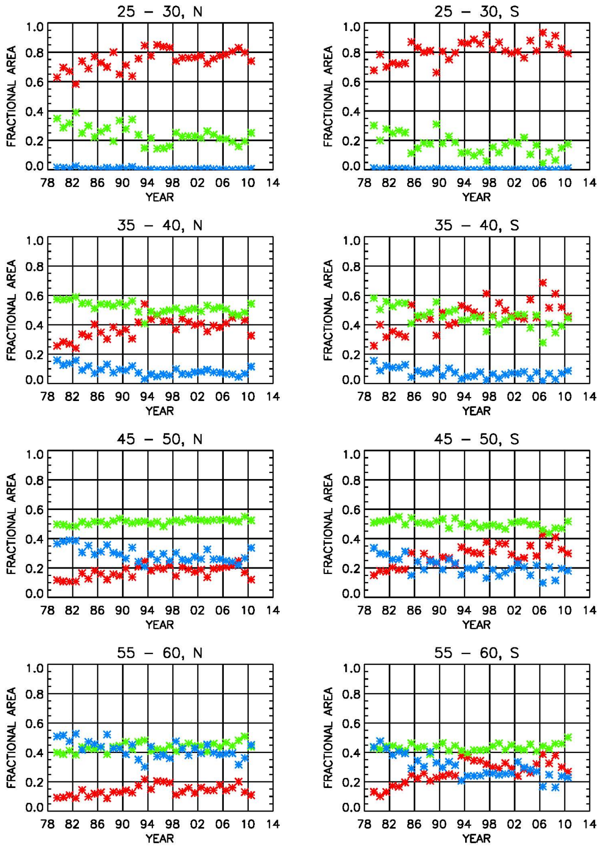

Fig. 7. The annual average fractional areas for the Tropical, mid-latitude, and Polar regimes versus time for both hemispheres, for 4 latitude bands. The Tropical regime is shown as the red stars; the mid-latitude regime as the green stars, and the Polar regime as the blue stars.

ACPD
11, 31067–31090, 2011

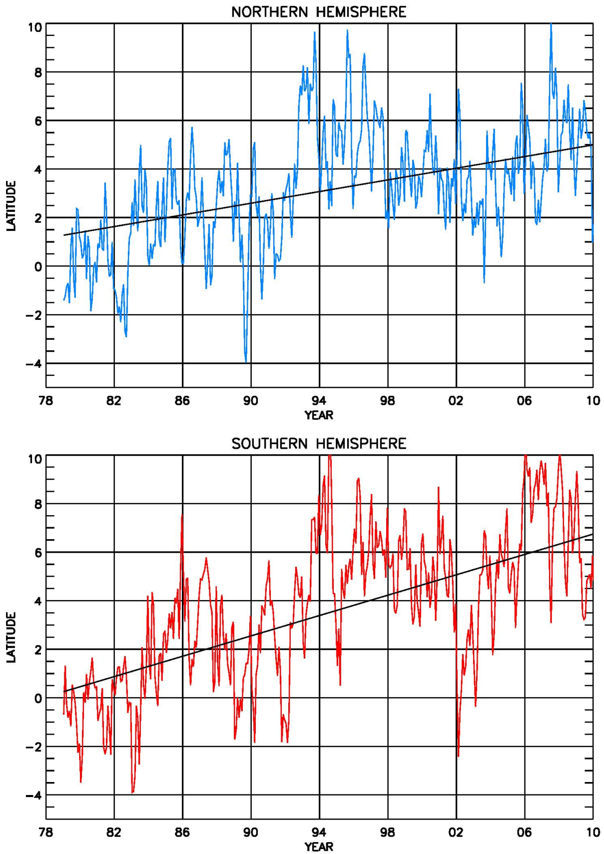

Fig. 8. Monthly mean equivalent latitude versus time for the subtropical front after the seasonal and QBO contributions have been removed. The solid black line shown for each hemisphere is the result of a linear fit, including measurement errors, to the revised data.

ACPD
11, 31067–31090, 2011

Measurements of the movement of the jet streams at mid-latitudes

R. D. Hudson